Applied Physics Letters ARTICLE scitation.org/journal/apl

Multisensory graphene-skin for harsh-environment applications

Cite as: Appl. Phys. Lett. **117**, 074101 (2020); doi: 10.1063/5.0017769
Submitted: 9 June 2020 · Accepted: 24 July 2020 ·
Published Online: 17 August 2020

Sohail F. Shaikh[1] and Muhammad M. Hussain[1,2,a)]

AFFILIATIONS

[1]mmh Labs, Electrical Engineering, King Abdullah University of Science and Technology (KAUST), Thuwal 23955-6900, Saudi Arabia
[2]EECS, Cory Hall, University of California Berkeley, California 94720-1770, USA

[a)]**Author to whom correspondence should be addressed:** muhammad.hussain@kaust.edu.sa and mmhussain@berkeley.edu

ABSTRACT

Monitoring the environment using electronic systems in harsh environments requires materials and processes that can withstand harsh environments. Environmental harshness can come from the surrounding temperature, varying pressure, intense radiation, reactive chemicals, humidity, salinity, or a combination of any of these conditions. Here, we present graphene as a candidate for a multisensory flexible platform in harsh-environment applications. We designed sensors for harsh environments like high temperature (operating range up to 650 °C), high salinity, and chemical harsh environments (pH sensing) on a single flexible polyimide sheet. The high-temperature graphene sensor gives a sensitivity of 260% higher than the Pt-based sensor. The temperature sensor acts between metal and a thermistor, thereby providing an opportunity to classify the region depending on temperature (<210 °C linear and > 210 °C up to 650 °C as quadratic). Improved performances are observed for salinity and pH sensing in comparison with existing non-graphene solutions. The simple transfer free fabrication technique of graphene on a flexible platform and laser-induced graphene on a flexible polyimide sheet opens the potential for harsh-environment monitoring and multisensory graphene skin in future applications.

With progressive developments in the field of Internet of Things (IoT) and Internet of Everything (IoE), miniaturized sensors that can be integrated with all kinds of environments have gained significant attraction from researchers. One of the fundamental parameters playing an important role in all disciplines of life is temperature and hence forms an integral part of devices for health monitoring,[1–7] environmental monitoring,[8–12] artificial electronic-skin (e-skin),[13–15] and many more emerging applications. Most of the monitoring applications require multiple sensors integrated on a single platform, and hence, recent works combine temperature, pressure, salinity, humidity, proximity, and flow sensing on a single platform.[11,13,16] Generally, sensors rely on the change in specific physical, mechanical, or chemical properties of the active material to detect the change that also dictates the application of sensors. Flexible and stretchable electronics have recently enabled myriads of opportunities and emerging applications. Metals, metal oxides, and ceramics are trivially at the heart of sensors; however, they are limited naturally by their bulkiness, inflexibility, and fragility for use in emerging applications. Consequently, thin-film metals, graphene, carbon nanotube (CNT), and carbon fiber are used in naturally flexible polymeric materials like ECOFLEX, polyethylene terephthalate (PET), polyimide (PI), papers, and polydimethylsiloxane (PDMS) to make physically flexible and robust sensors that can be used for a variety of applications.[17–24]

Graphene is one of the most popular 2D materials since the first demonstration of exfoliation using micro-mechanical cleaving in 2004. It has been extensively studied for superior properties like high electron mobility, mechanical strength, optical properties, and thermal conductivity,[25–28] and more recently been explored for sensing applications. High-quality single-layer graphene (SLG) can be obtained using a relatively simple chemical vapor deposition (CVD) process.[29] Consequently, there have been hundreds of studies conducted on using graphene-based sensors and electronic devices focused on health monitoring applications. However, challenges of defect-free transferring on the flexible substrates continue to pose significant challenges in process integration. Besides, the reliability of interconnects on the metal/graphene/polymer interface hinders the ready adaptability. Consequently, an effective method of production of porous graphene films using laser irradiation called laser-induced-graphene (LIG) has recently emerged, which is promising.[22–24,30,31] The electrical conductivity of LIG contacts relies strongly on the degree of photo-thermal

laser ablation of the material, which is dependent on the lasing output power during scribing.[32]

Despite having reported excellent electrical, mechanical, and thermal properties, graphene as sensing materials for emerging applications in harsh environments has not been explored significantly. Electronic devices used in harsh environments must be designed to withstand extreme conditions like extreme low or high temperatures, high radiation, high salinity, high pressure, or any other environment deviant from normal working surroundings. Temperature is one of the most critical parameters that can alter the electronic properties influencing their performance. Hence, it is important to choose the materials for harsh environments that are suitable for specific applications like marine environment monitoring (highly saline), space explorations (high temperature), and chemically harsh environments.[20] Graphene has been known to have superior properties such as a high electron mobility of 200 000 cm^2 $(V\ s)^{-1}$, an outstanding thermal conductivity in the range of 2000–5300 $W\ m^{-1}\ K^{-1}$, a high specific surface area of 2600 $m^2 g^{-1}$, and very high Young's modulus around 1000 GPa.[25,33–35] These properties lead to demonstrations of graphene as an active material for sensing applications (gas, flow, pressure, humidity, and temperature), in addition to the active electronic devices.[18,30,36] However, these are individual sensing applications and lack multisensory integration. Furthermore, these superior properties, which can make graphene an indispensable material choice for the harsh environment sensing applications, have been underexplored. Hence, we present here a graphene-based flexible multisensory platform that can be used in harsh environments to monitor high-temperature, conductivity (salinity), and pH of the medium. We first demonstrate CVD-grown SLG and LIG for high-temperature sensing applications using a simple transfer free fabrication process followed by device characterization for salinity and pH measurements.

We use two approaches to fabricate the multisensory graphene skin platform as illustrated in Fig. 1. Chemical vapor deposition (CVD) of graphene on the copper foil is a well-established method now to obtain high-quality thin graphene.[29,37] Typically, the grown graphene is transferred on the final substrate using polymer-assisted transfer techniques; however, adhesion, establishing contacts, patterning, and damage-free transfer remain major challenges for flexible substrates. Here, we use a transfer-free process in which high-quality graphene on a 25 μm thick Cu foil (from Graphenea^{TM}) is initially patterned using lithography and then etched with nitric acid (69% diluted in DI water) for 2 min. The obtained SLG on Cu foil was already flat and adhered to the Petri dish, which eliminates the wrinkles and damage during spin coating. However, if it is grown and the foil has wrinkles, then first, it shall be gently pressed using a glass slide to make it flat without extensive damage and a temporary carrier wafer with ecoflex/PDMS spin-coated and cured on it can be used as a host to process lithography and other steps. Other techniques of laser scribing or dry etching can also be applied to pattern the thin graphene. For the majority of flexible electronics applications, PDMS, PI, or Ecoflex materials are used as a final substrate, which are usually available in solution form. We spin the final flexible polymer PDMS (Sylgard^{TM} 184) mixed at the ratio of 1:10 (curing agent to the elastomer) directly on this patterned foil and cure at 60 °C for 90 min. This low-temperature direct curing allows good binding of the patterned foil with the PDMS substrate, while supporting copper is chemically etched using Iron(III) nitrate or ferric nitrate (nonahydrate solution prepared by mixing granules in de-ionized water (DI water) at the ratio of 1:3 by weight). Thus, a transparent multisensory graphene skin (G-skin) [Fig. 1(a) bottom left inset] was achieved on a flexible PDMS substrate without any transfer method involved.

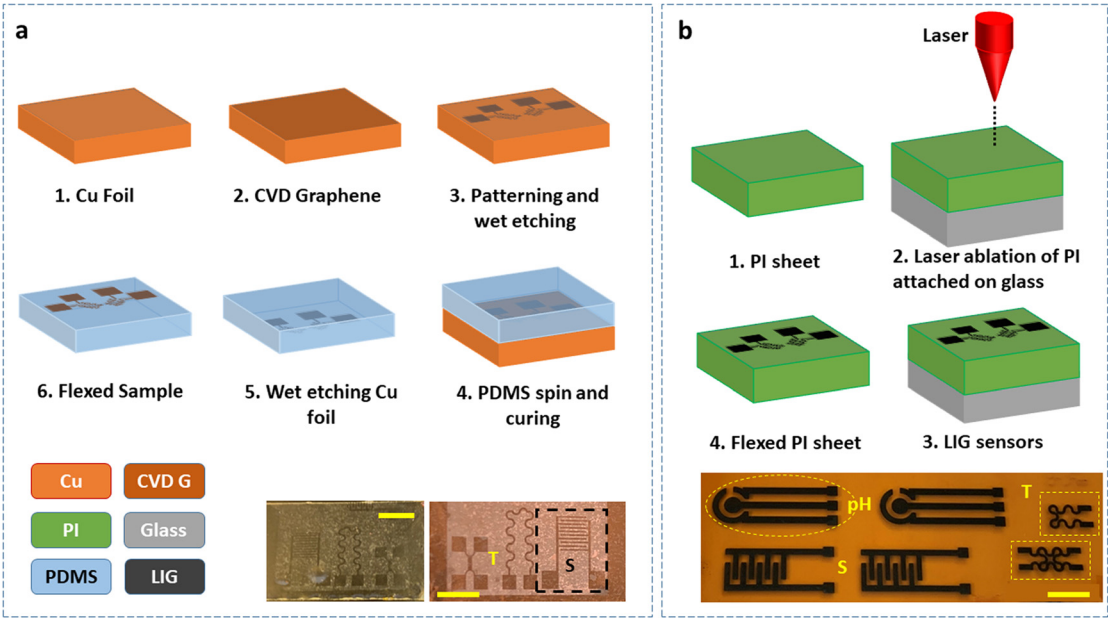

FIG. 1. Transfer free fabrication of graphene sensors on (a) PDMS as a final substrate (the right inset image shows the patterned sensors on Cu after patterning graphene, and the left image shows transparent flexible sensors on PDMS) and (b) laser-induced graphene (LIG) sensors on PI. The scale bar is 4 mm.

Although PDMS is a preferable material for many harsh environments where chemical, mechanical, and material stabilities are needed in addition to flexibility, it is not suitable for temperatures higher than 250 °C. On the contrary, PI is mechanically and thermally very stable material and also used heavily in flexible electronics as a substrate material. We can apply a similar process to obtain graphene on PI; however, graphene has very poor adhesion with PI that can be easily washed off and difficult to notice on the PI substrate unlike clearly visible structures on PDMS and SiO_2 substrates.

Hence, we adopted laser ablation to form LIG-based sensors using a CO_2 laser on a thick (125 μm) PI sheet (DuPont™ Kapton® HPP-ST IM301446)[24,32,38] as illustrated in Fig. 1(b). First, the PI sheet is attached to a glass slide of appropriate size to keep the sheet flat during the ablation process. It is very critical to keep the surface flat, which allows having the overall substrate in the same z-plane (at fixed focus) for the laser beam during ablation. Having small air bubbles and wrinkles can create minor focus shifts that are enough to produce errors during ablation like some portions will be properly focused forming graphene, while other parts may not (not carbonizing the PI sheet). Besides, the line widths (resolution of the lines) also depend on the focus in addition to the wavelength of the laser (here, the wavelength used is 10.6 μm). Thus, we have optimized critical parameters for forming LIG as 3.5% output power (maximum output power 6 W), 3% movement speed (~10 mm/s), 1000 PPI (pulses per inch), and a focused beam spot (working distance 3 mm).

Physical characterization of CVD graphene at different stages of the process and LIG were carried out using Raman spectroscopy and are compared in Fig. 2(a). From Raman spectroscopy, we have observed a very high-quality SLG profile where a 2D peak is higher than G in addition to having a negligible D peak that corresponds to the defects. We compared the conventional PMMA (polymethyl methacrylate)-assisted transfer method and our transfer free method for direct transfer on the flexible substrate, and we observed successful transfer of the film on both the rigid (SiO_2) and flexible substrate. Although we observed D peak enhancement in both cases that correspond to minor defects, these are not significant. Similarly, the Raman spectra of LIG represent higher defects compared to SLG, while D and G peaks are comparable to the 2D peak, revealing that LIG is thicker and a multilayer graphene structure. 2D peaks were observed to be around 2700 cm^{-1} with a negligible Raman shift across all the compared graphene material with the G peak around 1590 cm^{-1}. Furthermore, D peaks were observed to show relatively large shifts

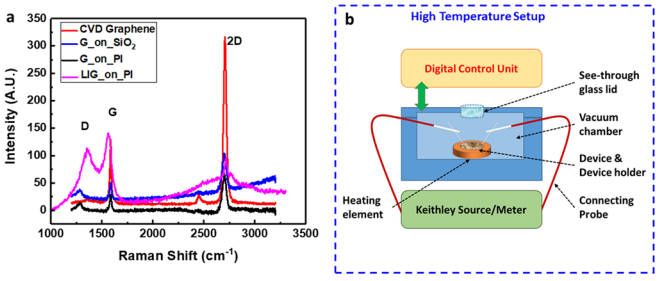

FIG. 2. (a) Physical characterization of CVD graphene on different substrates and LIG using Raman spectroscopy. Pronounced 2D peaks for CVD graphene at different stages show high quality with fewer defects on transfer compared to LIG. (b) Experimental setup for high-temperature sensor characterization.

from 1350 cm^{-1} for CVD graphene before transfer to ~1280 cm^{-1} for both transferred layers on SiO_2 and PI and ~1350 cm^{-1} for LIG. This implies a possible introduction of defects in the samples, which can be advantageous for sensing applications whereas not suitable for use as active electronic material.

Typically, when graphene is used as active material in biosensors or electrochemical sensors, they are for one-time use only. This is mainly due to the functionalization and presence of specific enzymes/biomarkers for a specific application. Here, we use it as a physical sensing device where its conductive material property is used as a replacement as metallic conductors. The multisensory platform hosts three kinds of sensing capabilities: temperature, conductivity (salinity), and pH of the solution, and show promising performance. The same flexible structure can also be used in microelectromechanical (MEMS)-based applications as a wearable multisensory platform for health monitoring and fitness tracking.

Most of the widely used temperature sensors are resistive temperature detectors (RTDs) having a typical fast response, high stability, and high accuracy. These RTDs have a metal (like platinum) that responds with increased resistance to increasing temperature. Here, we have used graphene-based RTDs for high-temperature environment applications with the added flexibility of the device. Two variations of temperature sensors were fabricated (Fig. 1) with 2 and 4 contact pads to have reliable measurement techniques, in which the four-wire measurement method counters the possible effects of resistance from the connecting leads. The design of the RTD temperature sensor resembles a serpentine shape widely reported in stretchable applications.[8,39] High-temperature characterization was performed in a high-temperature probe station with a vacuum chamber as shown in the experimental setup shown in Fig. 2(b). The temperature of the heating element that holds the device located inside the closed vacuum chamber can be controlled using a digital control box. The device is placed on the heating element and connected externally to a source/meter Keithley™ using high-temperature connecting probes. For consistency of measurements, we have kept the constant voltage source 1 V across the device and recorded the corresponding changes in the resistance as the temperature is increased from room temperature to 700 °C at 10 °C/min. A Pt-based temperature sensor was also fabricated on the PI sheet for comparison with the SLG temperature sensor. Pt was chosen due to its common usage in many commercial RTD-based temperature sensors.

From Fig. 3(a), we can observe that both Pt and SLG respond fast and withstand a high-temperature range. We observed a spike in the measurement when the temperature goes beyond 630 °C in both the cases, which is evidence of substrate breakdown (or meltdown) and hence device failure above this temperature. It is evident from the plot that the overall change in resistance for the overall temperature range for Pt-based temperature sensors (room temperature 25–630 °C) is very less compared to that of SLG. This means that the sensitivity of Pt-based sensors is ~0.31 Ω/°C with a linear response. Most of the metals show a linear response to temperature, while thermistors (mostly semiconductors) show non-linear (typically exponential) responses. For SLG-based sensors, we have observed two types of responses, linear response in the temperature range < 210 °C and quadratic response proportional to T^2 in the range > 210 °C. The resistance of a device is defined by the conduction of electrons; the number of electrons increases with an increase in temperature, thereby

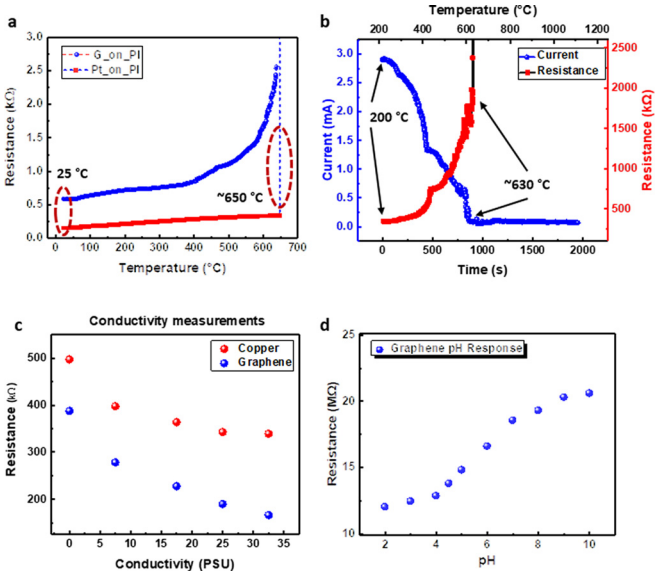

FIG. 3. Multisensory graphene-skin characterization: (a) high-temperature SLG sensor response to increasing temperature and (b) I–R response of LIG-based high-temperature sensor; both SLG and LIG show substrate breakdown around 630 °C. (c) Conductivity (salinity) sensor in comparison to the thin metal copper-based salinity sensor,[10] and (b) pH sensor response to pH buffer solutions.

reducing the overall mobility. The electrical conductivity of SLG has been known to be proportional to the carrier density and electron mobility, which are temperature-dependent that can be written as $\sigma = 1/\rho = qn\mu$, with q-charge, n-carrier density, and μ-mobility of the mobile charges. Also, the mobility depends on various scattering mechanisms such as defects, high-temperature annealing-induced doping, phonons, surfaces, and the interface between the substrate and graphene. For single-layer graphene, carrier density n has been reported to be proportional to T^2 at higher temperatures. Moreover, disorders are introduced in graphene with the defects at the interface increasing at high temperatures due to the annealing process. These are more prevalent and significant when metal/graphene contacts are established.[25,40–43] All these combined effects make the graphene temperature sensor switch from the linear region to the quadratic response at higher temperatures.

The sensitivity of the sensors can be deduced from the slope (resistance changeover external temperature change) of the linear response. However, for the quadratic response, we can take the average of resistance change after normalizing the resistance. Thus, the fabricated Pt sensor shows a linear response with a sensitivity of 0.311 Ω/°C, whereas sensitivity increases to 0.8356 Ω/°C (~260% higher than that of the Pt sensor) for the SLG temperature sensor in the linear regime (<210 °C) ($R^2 \sim 0.991$). This increased sensitivity can be attributed to the higher resistance change and increased electron density in SLG. We have repeated the experiments with the LIG temperature sensor for a higher temperature range of > 210 °C and observed similar patterns shown in Fig. 3(a), having a quadratic T^2 dependence with $R^2 \sim 0.9871$. Although a slight shift in the response was noticed for both SLG and LIG around 450 °C, it was not significant enough to be taken as another regime. The normalized resistance sensitivities for SLG and LIG before (in the range of 210–450 °C) and after (>450 °C) the shift were observed to be 1.829, 1.998, and 2.009/°C, respectively, concluding that the shift around the temperature is insignificant. Since LIG showed higher sensitivity, we have conducted other device characterization studies using LIG for salinity and pH measurements at room temperature. The characterization of these devices at elevated temperatures is not necessary as saline and chemical environments itself contribute as a harsh environment for the sensors.

Recently, there has been increasing interest in monitoring the ocean environment, which is another kind of harsh environment that demands specialized sensors and communication systems for underwater monitoring applications.[10,11,38] Seawater consists of different elements that help in maintaining and sustaining the marine life and ecosystem. Each element has a defining effect on the sustenance of ocean life. Conductivity (salinity) is one of the critical elements that regulate marine life behavior, and hence, the majority of biologging devices used for marine life explorations measure temperature, depth, and conductivity (salinity). There have been recent demonstrations of devices for such measurements using a flexible sensing platform, unlike trivial bulky, heavy, and invasive data logging devices. Here, we fabricated an interdigitated graphene conductivity sensor to measure the conductivity of the medium adapted from one of the recent demonstrations for the conductivity measurement and have achieved improved results. The conductive solutions were prepared manually in the lab by mixing different concentrations of salt in DI water, resulting in solutions ranging from 0 to 40 PSU (practical salinity unit), and compared the response. We have observed that the response of LIG-based conductivity sensors show a similar response to the increase in salinity by decreasing the resistance between the electrodes due to ionic conduction through the medium [Fig. 3(c)]. We have observed ~95% more sensitivity in LIG-based conductivity sensor than thin-metal based design (6.81 kΩ PSU^{-1} vs 4.87 kΩ PSU^{-1}) previously reported. The sensitivity can further be increased by having more fingers and reducing the spacing between fingers in the interdigitated pattern. Furthermore, copper is prone to easy oxidation and corrosion under normal conditions as well. Thus, graphene can serve as a better alternative for marine environment applications as well.

The human body can also be considered as a harsh environment as biofluids inside the body pose constraints on the implantable devices. Tremendous research activities are going for designing wearable and implantable physiological monitoring devices, and recently, pH sensing has become important using a variety of functional material and electrochemical approaches. Our pH sensor design resembles a potentiometric electrochemical sensor; however, the difference is in its passive performance (or physical sensing) unlike active material-based potentiometric pH sensors that can be used only once. The two electrodes adjacent to the central electrode are used for calibration and reducing the noise in the measurements. We used a small 3D-printed cube well and attached it to the area of interest on the sensor using uncured PDMS and let it cure at a low temperature of 60 °C for 1.5 h. This well is to contain the medium (solution) for which the pH is measured. pH solutions were prepared by adding buffer solutions in the DI water, and the corresponding resistance change was observed due to the change in the pH of the medium. We have manually added and removed the solution, and hence, the discrete readings can be observed in Fig. 3(d). A consistent increase in the resistance is observed as the

pH increases from 2 to 10. Although we have not observed a perfectly linear or quadratic (exponential) relationship, from the plot, we can conclude it to be discretely linear or linear in multiple regimes. We believe that this can be attributed to the errors in manual experimentation where solution residues may remain even after proper cleaning off from the sample. If an overall linear trendline is interpolated from the recordings, then the linear response shows the sensitivity of 1.257 MΩ ± 0.087 MΩ/pH with a coefficient of determination (COD) $R^2 = 0.963$ fairly close to unity for establishing a linear response.

A flexible multisensory platform (graphene-skin) is demonstrated using graphene for sensing applications in harsh-environment conditions. High-temperature, conductivity (salinity), and pH sensors were fabricated on a flexible polymer substrate (PDMS and PI) sheet using two different easy to follow approaches of transfer free flexible SLG graphene on the polymer and laser scribing-based LIG. Electrical characterization of the high-temperature sensor revealed that we can use graphene as a temperature sensor for a high-temperature environment (up to 650 °C), which was limited by the thermal limits of the polymer substrate only. Combining the standard technique of polymer-assisted transfer and converting silicon (or other materials that withstand high temperatures like SiC and GaN) into a flexible substrate, this range of operation can be further increased. SLG and LIG-based temperature sensors showed two distinct regions of operation when used for temperature sensing, linear behavior for temperatures <210 °C, and thermistor-like behavior for higher temperatures. This property can be used for a variety of interesting applications. The sensitivity observed for the linear region was found to be ∼260% higher than standard Pt-based RTD, establishing the better choice material. Also, salinity and pH sensors for an ocean-like harsh-environment have been reported here with improved performances compared to the existing metallic counterparts recently reported.

We believe that graphene has huge potential for exploring further emerging applications in harsh environments. Additionally, direct integration of sensors with the acquisition system will play a key role in monitoring applications, where heterogeneous materials, processes, and designs can be seamlessly integrated on a single platform to give a standalone system.

This publication is based upon the work supported by the King Abdullah University of Science and Technology (KAUST), Office of Sponsored Research (OSR), under Award No. REP/1/2707-01-01.

DATA AVAILABILITY

The data that support the findings of this study are available from the corresponding author upon reasonable request.

REFERENCES

[1]W. Gao, S. Emaminejad, H. Y. Y. Nyein, S. Challa, K. Chen, A. Peck, H. M. Fahad, H. Ota, H. Shiraki, D. Kiriya, D.-H. Lien, G. A. Brooks, R. W. Davis, and A. Javey, Nature **529**, 509 (2016).
[2]S. Yang, Y. C. Chen, L. Nicolini, P. Pasupathy, J. Sacks, B. Su, R. Yang, D. Sanchez, Y. F. Chang, P. Wang, D. Schnyer, D. Neikirk, and N. Lu, Adv. Mater. **27**, 6423 (2015).
[3]Y. Khan, M. Garg, Q. Gui, M. Schadt, A. Gaikwad, D. Han, N. A. D. Yamamoto, P. Hart, R. Welte, W. Wilson, S. Czarnecki, M. Poliks, Z. Jin, K. Ghose, F. Egitto, J. Turner, and A. C. Arias, Adv. Funct. Mater. **26**, 8764 (2016).
[4]Y. Khan, A. E. Ostfeld, C. M. Lochner, A. Pierre, and A. C. Arias, Adv. Mater. **28**, 4373 (2016).
[5]A. M. Hussain, E. B. Lizardo, G. A. Torres Sevilla, J. M. Nassar, and M. M. Hussain, Adv. Healthcare Mater. **4**, 665 (2015).
[6]S. M. Khan, N. Qaiser, S. F. Shaikh, and M. M. Hussain, IEEE Trans. Electron Devices **67**, 249 (2020).
[7]A. M. Hussain and M. M. Hussain, Adv. Mater. **28**(22), 4219–4249 (2015).
[8]S. M. Khan, S. F. Shaikh, N. Qaiser, and M. M. Hussain, IEEE Trans. Electron Devices **65**(11), 5038–5044 (2018).
[9]J. M. Nassar, S. M. Khan, D. R. Villalva, M. M. Nour, A. S. Almuslem, and M. M. Hussain, npj Flexible Electron. **2**, 24 (2018).
[10]J. M. Nassar, S. M. Khan, S. J. Velling, A. Diaz-Gaxiola, S. F. Shaikh, N. R. Geraldi, G. A. Torres Sevilla, C. M. Duarte, and M. M. Hussain, npj Flexible Electron. **2**, 13 (2018).
[11]S. F. Shaikh, H. F. Mazo-Mantilla, N. Qaiser, S. M. Khan, J. M. Nassar, N. R. Geraldi, C. M. Duarte, and M. M. Hussain, Small **15**, 1804385 (2019).
[12]R. B. Mishra, S. F. Shaikh, A. M. Hussain, and M. M. Hussain, AIP Adv. **10**, 055112 (2020).
[13]J. M. Nassar, M. D. Cordero, A. T. Kutbee, M. A. Karimi, G. A. T. Sevilla, A. M. Hussain, A. Shamim, and M. M. Hussain, Adv. Mater. Technol. **1**, 1600004 (2016).
[14]J. Kim, P. Gutruf, A. M. Chiarelli, S. Y. Heo, K. Cho, Z. Xie, A. Banks, S. Han, K. I. Jang, J. W. Lee, K. T. Lee, X. Feng, Y. Huang, M. Fabiani, G. Gratton, U. Paik, and J. A. Rogers, Adv. Funct. Mater. **27**(1), 1604373 (2017).
[15]A. J. Bandodkar, D. Molinnus, O. Mirza, T. Guinovart, J. R. Windmiller, G. Valdés-Ramírez, F. J. Andrade, M. J. Schöning, and J. Wang, Biosens. Bioelectron. **54**, 603 (2014).
[16]N. El-Atab, R. Almansour, A. Alhazzany, R. Suwaidan, Y. Alghamdi, W. Babatain, S. F. Shaikh, S. M. Khan, N. Qaiser, and M. M. Hussain, Small **16**, 1905399 (2020).
[17]L. Manjakkal, S. Dervin, and R. Dahiya, RSC Adv. **10**, 8594 (2020).
[18]S.-Y. Jeong, Y.-W. Ma, J.-U. Lee, G.-J. Je, and B. S. Shin, Sensors **19**, 4867 (2019).
[19]Y. Yang, Y. Song, X. Bo, J. Min, O. S. Pak, L. Zhu, M. Wang, J. Tu, A. Kogan, H. Zhang, T. K. Hsiai, Z. Li, and W. Gao, Nat. Biotechnol. **38**, 217 (2020).
[20]A. S. Almuslem, S. F. Shaikh, and M. M. Hussain, Adv. Mater. Technol. **4**, 1900145 (2019).
[21]P. Miao, J. Wang, C. Zhang, M. Sun, S. Cheng, and H. Liu, *Graphene Nanostructure-Based Tactile Sensors for Electronic Skin Applications* (Springer, Singapore, 2019).
[22]M. G. Stanford, K. Yang, Y. Chyan, C. Kittrell, and J. M. Tour, ACS Nano **13**, 3474 (2019).
[23]L.-Q. Tao, H. Tian, Y. Liu, Z.-Y. Ju, Y. Pang, Y.-Q. Chen, D.-Y. Wang, X.-G. Tian, J.-C. Yan, N.-Q. Deng, Y. Yang, and T.-L. Ren, Nat. Commun. **8**, 14579 (2017).
[24]J. Lin, Z. Peng, Y. Liu, F. Ruiz-Zepeda, R. Ye, E. L. G. Samuel, M. J. Yacaman, B. I. Yakobson, and J. M. Tour, Nat. Commun. **5**, 5714 (2014).
[25]B. Davaji, H. D. Cho, M. Malakoutian, J.-K. Lee, G. Panin, T. W. Kang, and C. H. Lee, Sci. Rep. **7**, 8811 (2017).
[26]F. Bonaccorso, Z. Sun, T. Hasan, and A. C. Ferrari, Nat. Photonics **4**, 611 (2010).
[27]C. Lee, X. Wei, J. W. Kysar, and J. Hone, Science **321**, 385 (2008).
[28]K. I. Bolotin, K. J. Sikes, Z. Jiang, M. Klima, G. Fudenberg, J. Hone, P. Kim, and H. L. Stormer, Solid State Commun. **146**, 351 (2008).
[29]M. T. Ghoneim, C. E. Smith, and M. M. Hussain, Appl. Phys. Lett. **102**, 183115 (2013).
[30]M. Marengo, G. Marinaro, and J. Kosel, in Proceedings of the IEEE Sensors (2017), Vol. 1.
[31]A. Kaidarova, N. Alsharif, B. N. M. Oliveira, M. Marengo, N. R. Geraldi, C. M. Duarte, and J. Kosel, Global Challenges **4**, 2000001 (2020).
[32]F. J. Romero, A. Rivadeneyra, A. Salinas-Castillo, A. Ohata, D. P. Morales, M. Becherer, and N. Rodriguez, Sens. Actuators, B **287**, 459 (2019).
[33]J. Li, X. Y. Chen, R. B. Lei, J. F. Lai, T. M. Ma, and Y. Li, J. Mater. Sci. **54**, 7553 (2019).
[34]H. Huang, S. Su, N. Wu, H. Wan, S. Wan, H. Bi, and L. Sun, Front. Chem. **7**, 399 (2019).

[35]T. Gan and S. Hu, Microchim. Acta **175**, 1 (2011).
[36]A. F. Carvalho, A. J. S. Fernandes, C. Leitão, J. Deuermeier, A. C. Marques, R. Martins, E. Fortunato, and F. M. Costa, Adv. Funct. Mater. **28**, 1805271 (2018).
[37]R. Qaisi, C. Smith, and M. M. Hussain, in *2013 Saudi International Electronics, Communications and Photonics Conference* (IEEE, 2013).
[38]A. Nag, S. C. Mukhopadhyay, and J. Kosel, Sens. Actuators, A **264**, 107 (2017).
[39]S. F. Shaikh and M. M. Hussain, in *IEEE 5th World Forum Internet Things, WF-IoT 2019 Conference Proceedings* (IEEE, 2019), pp. 309–312.
[40]Y. Yin, Z. Cheng, L. Wang, K. Jin, and W. Wang, Sci. Rep. **4**, 5758 (2014).
[41]A. Akturk and N. Goldsman, J. Appl. Phys. **103**(5), 053702 (2008).
[42]T. Kaplas, V. Jakstas, A. Biciunas, A. Luksa, A. Setkus, G. Niaura, and I. Kasalynas, Condens. Matter **4**, 21 (2019).
[43]W. Xueshen, L. Jinjin, Z. Qing, Z. Yuan, and Z. Mengke, J. Nanomater. **2013**, 1 (2013).